The field integrated method to solve time domain electromagnetic problems

Zhifeng Sheng*, Rob Remis† and Patrick Dewilde*,
* Email: {Z.Sheng, P.Dewilde}@ewi.tudelft.nl
† Email: R.F.Remis@ewi.tudelft.nl

***Abstract*—This paper presents a survey and a number of experiments with the (relatively new) Integrated Field Equations method for Maxwell's equations. It starts out with a summary of the method, followed by a number of test cases in which its special properties, in particular its ability to handle high contrast using coarse grids is demonstrated. Numerical experiments show that the resulting algorithms are stable and achieve high quality field interpolation even in the presence of very high contrasts.**

***Index Terms*—least-squares, Surface Integrated Field Equations, time domain computational electromagnetism, hybrid finite element, high contrast**

I. METHOD OUTLINE

In strongly heterogeneous media, the constitutive parameters can jump by large amounts upon crossing the material interfaces. On a global scale, the EM field components are, therefore, not differentiable and Maxwell's equations in differential form cannot be used: one has to resort to the original integral form of the EM field relations as the basis for the computational method. The appropriate integral form is provided by the classical interrelations between the curl of the electric/magnetic field strength along a closed curve and the time rate of change of the magnetic/electric flux passing through a surface with the circulation loop as boundary. For these to hold, only integrability of the field is needed, which condition we impose in accordance with the physical condition of boundedness of the field quantities. To satisfy the constitutive relations (that are representative of physical volume effects), a fitting continuation of the boundary representations of the field components of an element into its interior is needed. We construct a consistent algorithm that meets all of these requirements, using a simplicial geometrical discretization combined with piecewise linear representation of the electric and magnetic field components along the edges of the elements, piecewise linear extrapolations into the interior of the elements and taking constant values of the constitutive coefficients in these interiors. Furthermore, we use NETGEN[4] to discretize the computational domain with a 2D(triangular)/3D(tetrahedra) mesh. We use simple boundary conditions (PEC, PMC) to truncate the computational domain. After properly assembling the local matrices, we obtain a symmetric positive definite system of algebraic equations, which we solve with a preconditioned iterative method. We test the accuracy of the method by comparing the computed solution with analytic solutions.

II. SURFACE INTEGRATED MAXWELL'S EQUATIONS

In the computation domain Ω with boundary $\partial\Omega$, given a (sufficiently smooth and small) surface S with boundary ∂S, Maxwell's equations in the surface integrated form are

$$\oint_{\partial S} H \bullet dl = \int_S \{\partial_t D + \sigma^e E + J^{imp}\} \bullet ds, \quad (1)$$

$$\oint_{\partial S} E \bullet dl = -\int_S \{\partial_t B + \sigma^m H + K^{imp}\} \bullet ds. \quad (2)$$

where $\sigma^e(x_r)$ is the electric conductivity, $\sigma^m(x_r)$ is the magnetic conductivity. Let $K^{tot} = \partial_t B + \sigma^m H + K^{imp}$, $J^{tot} = \partial_t D + \sigma^e E + J^{imp}$, consider a volume V with its closed surface ∂V, The compatibility relations in their integrated form are:

$$\oint_{\partial V} J^{tot} \bullet ds = 0, \quad (3)$$

$$\oint_{\partial V} K^{tot} \bullet ds = 0. \quad (4)$$

The computational domain is truncated by PEC and PMC boundary conditions:

$n \times E = 0$ on $\partial\Omega_1$, $n \bullet K^{tot} = 0$ on $\partial\Omega_1$ (PEC boundary),
$n \times H = 0$ on $\partial\Omega_2$, $n \bullet J^{tot} = 0$ on $\partial\Omega_2$ (PMC boundary).

where $\partial\Omega_1 \cap \partial\Omega_2 = \phi$, $\partial\Omega_1 \cup \partial\Omega_2 = \partial\Omega$; Last but not the least, the interface conditions are:

$$[n \bullet K^{tot}] = 0 \text{ on } \Gamma_i, \quad [n \times H] = 0 \text{ on } \Gamma_i,$$
$$[n \bullet J^{tot}] = 0 \text{ on } \Gamma_i, \quad [n \times E] = 0 \text{ on } \Gamma_i.$$

where $[A] = \lim A(\Gamma^+) - \lim A(\Gamma^-)$ denotes the jump of a quantity A across the material interface Γ. The constitutive relations are:

$$D(x_r, t) = \varepsilon(x_r) E(x_r, t), \quad B(x_r, t) = \mu(x_r) H(x_r, t).$$

where $\varepsilon(x_r)$ is the permittivity, $\mu(x_r)$ the permeability.

III. DISCRETE SURFACE INTEGRATED FIELD EQUATIONS FOR TWO DIMENSIONAL (PERPENDICULAR POLARIZATION) PROBLEM

The 2D problem is characterized by invariance in the z direction. With the additional assumption that the media is time invariant, isotropic and instantaneously locally reacting, the EM field can be decoupled into a parallel polarization case and a perpendicular polarization case. For the perpendicular polarization case, the magnetic field strength is interpolated with hybrid linear finite elements while the electric field strength is interpolated with nodal linear finite elements. The continuity properties of field strengths are then fully preserved . Our discretization procedure is similar to that in [2], except that the discrete Maxwell's equations are derived there only for static problems, while we work on full Maxwell's equations in the time-domain. In the perpendicular polarization case, the tangential components of magnetic field strengths are continuous across the interfaces, therefore, magnetic field strength is approximated with edge based linear finite elements on material interfaces, and node linear finite elements in homogeneous sub-domains. The electric field pointing to the z direction is tangential to material interfaces, therefore always continuous; nodal linear finite elements are used to interpolate it. Other quantities are interpolated with nodal linear finite elements. Here we give a short survey on the discrete surface integrated equations, for details see [5]. Applying the equation (1) on the face delimited by points $i = P_1, j = P_2, k = P_3$ (see Fig.1), and approximate the line and surface integrals with trapezoidal rule. We get:

$$\begin{aligned}\frac{1}{2}l_i[H_k(t)\bullet e_{kj} + H_j(t)\bullet e_{kj}] + \frac{1}{2}l_j[H_i(t)\bullet e_{ik} + H_k(t)\bullet e_{ik}]&\\ +\frac{1}{2}l_k[H_j(t)\bullet e_{ji} + H_i(t)\bullet e_{ji}]&\\ +\frac{A}{3}[(\sigma^e_{izz} + \varepsilon_{izz}\partial_t)E_{iz}(t) + (\sigma^e_{jzz} + \varepsilon_{jzz}\partial_t)E_{jz}(t)&\\ +(\sigma^e_{kzz} + \varepsilon_{kzz}\partial_t)E_{kz}(t)]&\\ = -\frac{A}{3}[J^{imp}_{iz}(t) + J^{imp}_{jz}(t) + J^{imp}_{kz}(t)]& \quad (5)\end{aligned}$$

Where $H_l(t),\ l \in \{i, j, k\}$ may be represented by either nodal linear expansion or edge linear expansion. Apply the equation (2) on the face delimited by points $j = P_2, k = P_3, k' = P_6, j' = P_5$, and approximate the line and surface integrals with trapezoidal rule. We get:

$$E_{kz} - E_{jz} = -\frac{1}{2}l_i[K^{tot}_k\bullet a_i + K^{tot}_j\bullet a_i] \quad (6)$$

Apply and approximate the equation 2 on the face delimited by points $i = P_1, k = P_3, k' = P_6, i' = P_4$:

$$E_{iz} - E_{kz} = -\frac{1}{2}l_j[K^{tot}_i\bullet a_j + K^{tot}_k\bullet a_j] \quad (7)$$

Apply and approximate the equation 2 on the face delimited by points $j = P_3, i = P_2, i' = P_4, j' = P_5$. We get:

$$E_{jz} - E_{iz} = -\frac{1}{2}l_k[K^{tot}_j\bullet a_k + K^{tot}_i\bullet a_k] \quad (8)$$

The above semi-discrete equations are then integrated in time, where the trapezoidal rule is applied to approximate the integral in time. To maintain accuracy in the time-domain and avoid computing too many unnecessary time-steps, We choose the time-step δt corresponding to a CFL number between 1 and 2 for the smallest element (see [1]).

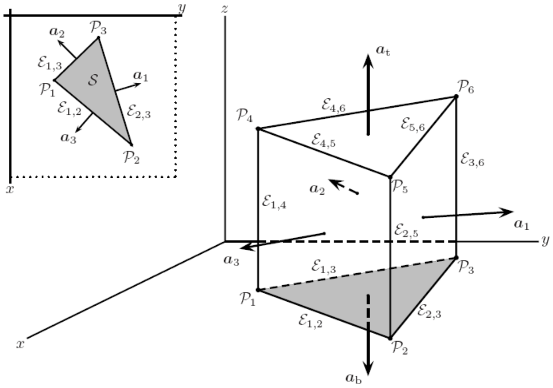

Fig. 1. The prism element.

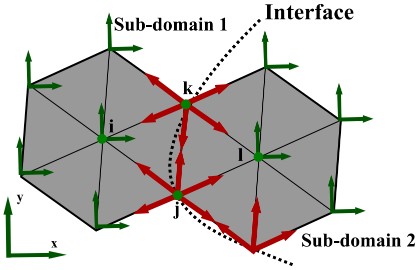

Fig. 2. The allocation of the nodal- and edge- linear finite elements.

A. Constitutive Relations

To determine the electromagnetic field strength, the constitutive relations are described via equations

$$K^{tot}(t) = \sigma^m H(t) + \mu\partial_t H(t) + K^{imp}(t) \quad (9)$$

assume the magnetic constitutive parameters are isotropic with respect to x and y direction, we have, for edge expansions:

$$\begin{aligned}K^{tot}_i(t) - (\sigma^m_i + \mu_i\partial_t)[H_{ij}(t)\frac{a_j}{e_{ij}a_j} + H_{ik}(t)\frac{a_k}{e_{ik}a_k}]&\\ = K^{imp}_i(t),&\\ i{\neq}j{\neq}k;\quad i, j, k \in \{P_1, P_2, P_3\}& \quad (10)\end{aligned}$$

and for nodal element:

$$\begin{aligned}K^{tot}_i(t) - (\sigma^m_i + \mu_i\partial_t)H_i(t) = K^{imp}_i(t),&\\ i \in \{P_1, P_2, P_3\}& \quad (11)\end{aligned}$$

To simplify the system to be solved, we substitute the consititutive relations into equations (6-8) and eliminate unknown $K^{tot}_i(t)$.

B. Discrete interfaces conditions

For nodal finite elements, the tangential component as well as the normal component are continuous, therefore, there is no need for enforcing interface conditions on nodal finite elements. For linear edge finite elements, we need to enforce the interface condition $[n\bullet K^{tot}] = 0$ on Γ_i, tangential continuity is satisfied automatically by the discrete magnetic field. The interface conditions are to be enforced point-wise-ly. Suppose point j and k are on the interface Γ_i, the edge jk is shared by two triangular finite elements $\Delta(i,j,k)$ and $\Delta(j,l,k)$ on both sides of Γ_i as shown in Figure 2. The following equation enforces the interface condition on point j:

$$\begin{aligned} &\mu_j^- \frac{a_i \bullet a_i}{e_{ji} \bullet a_i} H_{ji}(n+1) + \mu_j^- \frac{a_i \bullet a_k}{e_{jk} \bullet a_k} H_{ji}(n+1) \\ &+\mu_j^+ \frac{a_l \bullet a_l}{e_{jl} \bullet a_l} H_{jl}(n+1) + \mu_j^+ \frac{a_l \bullet a_k}{e_{jk} \bullet a_k} H_{jk}(n+1) \\ &\quad = \mu_j^- \frac{a_i \bullet a_i}{e_{ji} \bullet a_i} H_{ji}(n) + \mu_j^- \frac{a_i \bullet a_k}{e_{jk} \bullet a_k} H_{ji}(n) \\ &\quad +\mu_j^+ \frac{a_l \bullet a_l}{e_{jl} \bullet a_l} H_{jl}(n) + \mu_j^+ \frac{a_l \bullet a_k}{e_{jk} \bullet a_k} H_{jk}(n) \end{aligned} \tag{12}$$

μ_j^- is the permeability in $\Delta(i,j,k)$ and μ_j^+ is the permeability in $\Delta(j,l,k)$. Note that, the enforcing of the pointwise interface condition is not always necessary, because the interfaces conditions are actually enforced in its integral form by the discrete integrated field equations (Add the surface integrated field equations for edge jk in $\Delta(i,j,k)$ and in $\Delta(j,l,k)$, and you will get the corresponding interface condition on edge jk in its integral form). The pointwise interface conditions are enforced to make sure the global system has full column rank and to improve the condition number of the least-squares system. The same kind of equation will be set for point k, the global discrete interfaces conditions $Wu(n+1) = Wu(n)$ is a row-wise collection of these point-wise-ly discrete interface conditions.

IV. THE LINEAR SYSTEM AND PRECONDITIONED CG-LIKE METHOD

After least-squares formulation, we have the spatially and temporally discrete linear system:

$$A_2 u_i = -A_1 u_{i-1} + G_i \tag{13}$$

where u_{i-1} collects the solution of the previous time instance, $u_i = \left[\begin{array}{cc} H_i & E_i \end{array}\right]^H$ collects the solution of the current time instance. G_i collects the source terms and boundary terms. u_0 collects the initial field strength. Due to the least-squares formulation, A_2 is symmetric positive definite. In fact, one of the main appealing features of the least-squares method is that it always leads to the solution of a symmetric positive definite system. The symmetric positive definite system can be solved via any preconditioned Krylov space iterative solution method. Good preconditioners are needed in iterative solution methods. The preconditioner we used is the incomplete Cholesky factorization (IC). The incomplete Cholesky factorization with dropping threshold 10^{-3} ($IC(10^{-3})$) works very generally and improves iterative convergence a lot; however, direct application of $IC(10^{-3})$ on the matrix A_2 would introduce a lot of fill-ins to the incomplete Cholesky factor. Applying the approximate symmetric minimum degree ordering [3] on the matrix A_2 will reduce the fill-ins of the incomplete Cholesky factor significantly. Then preconditioned Krylov space iterative solvers can be used to solve the symmetric positive definite matrix. The solution method normally takes less than 10 iterations to reach accuracy 10^{-6}. Fewer iterations are needed if the solution of the previous time instance is taken as the initial guess of the current time instance.

V. NUMERICAL EXPERIMENT

We test our method on sample examples for which an analytic solution is available. Experiments show that our solution should follow the actual theoretical steady state solution faithfully. the computed solution stays stable and the error divergence of our method is much lower than with that computed with the classical nodal method using the same coarse mesh.

A. *Homogeneous configuration*

We test our method on a time domain example where analytic solution exists. The configuration is a square domain $\Omega = \{0 \leq x \leq 1, 0 \leq y \leq 1\}$ consisting of vaccum ($\epsilon_r = 1, \mu_r = 1, \sigma^e = 0, \sigma^m = 0$). The computational domain is surrounded by PEC boundary. The source densities are given by:

$$J_z^{imp} = A\sin(\omega t)\delta(x-0.5)\delta(y-0.5) \tag{14}$$

$$K_x^{imp} = 0 \tag{15}$$

$$K_y^{imp} = 0 \tag{16}$$

Where $\omega = 2\pi f$, the frequency f is 1GHZ, the wave length $\lambda = c0/f = 0.3m$, $A = 1000$. Assuming the interesting time interval is short enough such that effect of the boundaries does not affect the solution, the analytic solution for electric field strength is known in closed form as:

$$E_z(x,y,t) = \begin{cases} 0, & t < T \\ -\frac{\mu_0}{2\pi}\int_{\tau=T}^{t} \frac{\partial_t J_z^{imp}(t-\tau)}{\sqrt{\tau^2 - T^2}} d\tau, & t > T \end{cases} \tag{17}$$

To deal with the singularity at $\tau = T$, let $u = T\cosh(\tau)$, electric field strength can be written as:

$$E_z(x,y,t) = \begin{cases} 0, & t < T \\ -\frac{\mu_0}{2\pi}\int_{u=0}^{\text{acosh}\frac{t}{T}} A\omega\sin(\omega t - \omega T\cosh(u)) du, & t > T \end{cases}$$

where $T = \sqrt{(x-0.5)^2 + (y-0.5)^2}/c_0$ is the arrival time for the wave to travel from the source location to the observation location. In our finite element approximation, the spacial delta function is approximated with linear finite element approximation. Therefore, the analytic solution will have to be weighted over that domain. We pick the observation point $(x,y) = (0.6, 0.5)$ and compared the computed solution on this point with the analytic solution in the time domain. The solutions computed with different mesh size and time step size are plotted in time domain in Fig.3 Snapshot of the electric field strength are shown in Fig.4. We can see that these simulation solutions agree with the exact solution very well (except the first few time steps). Consequently, we can say that we have a good solution, stable for a mesh size close to $\lambda/5$.

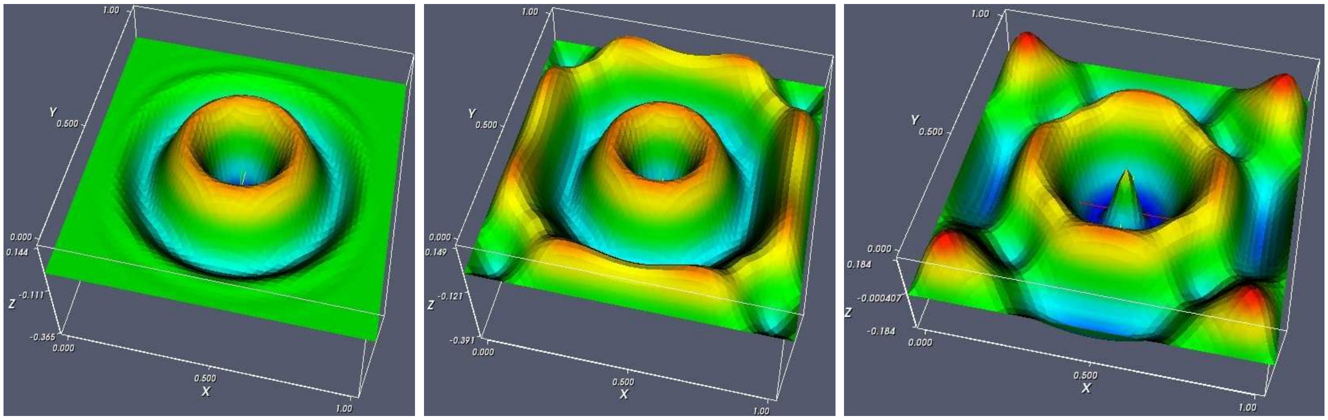

Fig. 4. The snapshots of the electric field strengths at $t_1 = 1.23$ns, $t_2 = 2.17$ns, $t_3 = 2.47$ns computed with the least-squares field integrated method.

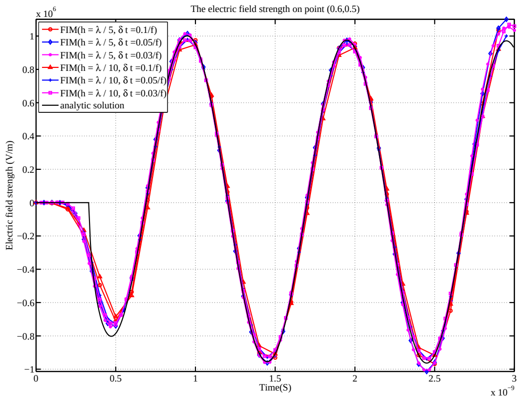

Fig. 3. The electric field strength on observation point $(0.6, 0.5)$ in time domain, analytic solution and the computed solutions with $h_1 = \lambda/5$, $h_2 = \lambda/10$ and $\delta t_1 = \frac{1}{10f} \approx 0.1$ns, $\delta t_2 = \frac{1}{20f} \approx 0.05$ns, $\delta t_3 = \frac{1}{30f} \approx 0.033$ns. The analytic solution is weighted over the discrete 2D delta function.

TABLE I
CONFIGURATION OF THE SECOND EXPERIMENT

Ω_i	Definition of sub-domains	μ_r	σ^m	ϵ_r	σ^e
Ω_1	$0 \le x < 1$ $0 \le y < 0.3$	1	0	2	0
Ω_2	$0.4 \le x \le 0.6$ $0.3 \le y < 0.4$	1	0	1	10^7
Ω_3	$\Omega - \Omega_1 - \Omega_2$	1	0	1	0

B. *High conductivity configuration*

We test our method on a more realistic example where high contrasts exist. We use zero vector as the initial state, and then start integrating from there in the time domain. The configuration is a square domain $\Omega = \{0 \le x \le 1, 0 \le y \le 1\}$ consisting of three sub-domains $\Omega_i, \{i = 1, 2, 3\}$ with different medium properties (See Table I). The computational domain is surrounded by PEC boundary. The source densities are given by:

$$\begin{aligned} J_z^{imp} &= -\chi(t)\sqrt{2\theta e}(t - t_0)\exp[-\theta(t - t_0)^2]\delta(x - 0.5)\delta(y - 0.7) \\ K_x^{imp} &= 0 \\ K_y^{imp} &= 0 \end{aligned}$$

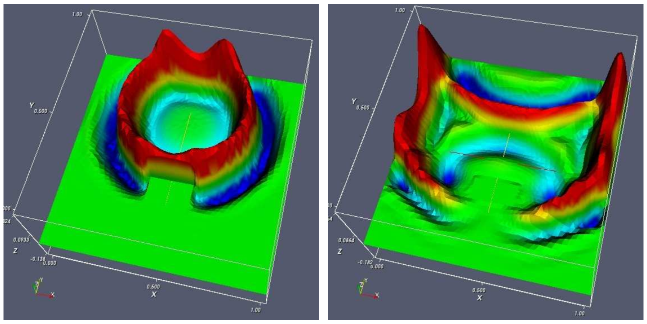

Fig. 5. The snapshot of electric field strength at $t_1 = 3$ns, $t_2 = 3.7$ns computed with $h = \lambda/10$, $\delta t = 0.033$ns

Where $\chi(t)$ is the heaviside step function, the peak frequency f_{peak} is 1GHZ, $t_0 = 2$ns, $\theta = 2\pi^2 f_{\text{peak}}^2$. the simulation is done in time domain. As always, edge- finite elements are used on interfaces only, nodal finite elements are used elsewhere. Snapshots of electric field strength computed with hybrid finite elements are shown in Fig. 5.

VI. CONCLUSION

The Least-squares field integrated method based on hybrid linear finite elements holds considerable promise to model electromagnetic effects in integrated circuits, where high contrasts between different types of materials is the rule and complex structures are present; however, more theoretical study as well as practical study are needed to utilize its advantages.

REFERENCES

[1] BO-NAN Jiang. *The Least-Squares Finite Element Method: Theory and Applications in Computational Fluid Dynamics and Electromagnetics (Scientific Computation)*, page 369. 2006.

[2] I. E. Lager. *Finite element modelling of static and stationary electric and magnetic fields*. PhD thesis, Delft University of Technology, 1996.

[3] T. A. Davis P. Amestoy and I. S. Duff. Amd, an approximate minimum degree ordering algorithm. *ACM Transactions on Mathematical Software*, 30:381–388, Sept 2004.

[4] J. Schoberl. Netgen - an advancing front 2d/3d-mesh generator based on abstract rules. *Comput.Visual.Sci*, 1:41–52, 1997.

[5] Zhifeng Sheng, Rob Remis, and Patrick Dewilde. A least-squares implementation of the field integrated method to solve time domain electromagnetic problems. *CEM-TD*, Oct 2007.